6-2020

Towards the Design of a Wideband Reflective Long Period Grating Distributed Sensor

Sohel Rana
Boise State University

Nirmala Kandadai
Boise State University

Harish Subbaraman
Boise State University

Publication Information

Rana, Sohel; Kandadai, Nirmala; and Subbaraman, Harish. (2020). "Towards the Design of a Wideband Reflective Long Period Grating Distributed Sensor". *Journal of Physics Communications, 4*(6), 065015-1 - 065015-8. https://dx.doi.org/10.1088/2399-6528/ab9dd6

Journal of Physics Communications

OPEN ACCESS

RECEIVED
1 May 2020

REVISED
12 June 2020

ACCEPTED FOR PUBLICATION
17 June 2020

PUBLISHED
26 June 2020

PAPER

Towards the design of a wideband reflective long period grating distributed sensor

Sohel Rana , Nirmala Kandadai and Harish Subbaraman

Department of Electrical and Computer Engineering, Boise State University, Boise, ID 83725, United States of America

E-mail: harishsubbaraman@boisestate.edu

Keywords: long period grating, metal coating, multi-parameter sensing

Abstract

In this paper, we computationally investigate the effects of metal coating length and coating coverage on the reflected spectrum of a long period grating (LPG) over a broad bandwidth. Simulation results indicate that coating the tail end of the fiber between the LPG and the end facet of the fiber provides a reflected spectrum that mimics the LPG transmission spectrum shape over a 400 nm bandwidth. Based on single LPG simulation results, we present the design of a distributed LPG structure containing a multiple number (n) of LPGs in reflection mode for the first time. Simulation results for $n = 1, 2$, and 3 are presented here to demonstrate the concept of a distributed reflective LPG design. It is expected that such a sensor will open a new window for distributed sensing using reflective LPGs.

1. Introduction

A long period grating (LPG) works on the principle of light coupling between the fundamental core mode and a number of co-propagating cladding modes [1–3]. Such coupling results in an LPG transmission spectrum with a number of discrete attenuation bands depending on the phase matching condition for a resonance wavelength (λ_m) given by [1]:

$$\lambda_m = (n_{eff,co} - n_{eff,cl}^m)\Lambda \quad (1)$$

where $n_{eff,co}$ is the effective refractive index of the guided core mode, $n_{eff,cl}^m$ is the effective refractive index of the m-th order cladding mode and Λ is the grating period. It can be seen from equation (1) that the resonance wavelengths are dependent on the grating period and the effective refractive indices of the core and the cladding modes.

Since external parameters, such as temperature, pressure, or a secondary medium in close proximity with the cladding can directly influence the effective indices of the cladding modes, the resonance wavelengths also respond to these changes. Thus, LPG sensors have found several potential applications in monitoring temperature, strain, and refractive index [4–8]. However, an LPG is limited in applications in that it can only be used as a transmission sensor, compared to a fiber Bragg grating (FBG) sensor which is convenient as a reflection mode sensor. From a packaging viewpoint, it is preferable to use the same facet for coupling light into and out of the fiber to maximize their applications [9].

To overcome the abovementioned limitation of a conventional LPG design, several LPG designs have recently been reported in literature that can operate in the reflection mode [10–14]. For example, in [11], an LPG based on the Michelson interferometer was investigated to collect light reflected from the end facet of fiber at the input facet. However, interferometric fringes containing reflected spectrum made data interpretation cumbersome. Then in [12], a reflective LPG containing a polymer microtip at the end facet that reflects select cladding modes was proposed. Although this reflective LPG was able to measure the refractive indices of water/glycerol solution, a complex fabrication process for polymer microtip using photo polymerization was utilized. In [14], a very compact reflective LPG that reflects light without interferometric fringes was reported. In this design, both the fiber end facet and the side of the fiber was coated with silver metal in order to obtain a reflected spectrum that mimicked the transmitted spectrum. The design and operation of the reflective LPG was limited

to within a narrow bandwidth around one of the resonance wavelengths, thus limiting the understanding of the use of the sensor across a wide bandwidth, specifically for distributed sensing applications. Additionally, the reflective LPG design used a very short length of end coating which was not optimized to completely mimic the transmission spectrum shape.

In this work, we show that—(1) the coating length, defined as length of the metal coating from the end facet of the fiber, and (2) the coating coverage, defined as the ratio of metal coating length over the LPG to the total length of the LPG, have a significant impact on the reflected spectrum over a wide bandwidth. Using these results, we present an optimized design for reflective distributed LPG structure comprising of n number of LPGs with different periods in a single fiber that entirely mimics the transmission spectrum over a wide bandwidth for the first time.

2. Geometric structure of a distributed reflective LPG

A schematic diagram of the proposed distributed sensor design comprising of cascaded reflective LPGs is shown in figure 1. The grating period of the n-th LPG is denoted by Λ_n. L_c denotes the coating length, L_{gn} is the length of n-th LPG, L_{end} is the length of the tail end of the fiber measured from the end facet to the end of the n-th LPG, d_i is the distance between two adjacent LPGs. In this design, we used gold as the metal coating the fiber. Please note that in all of the cases considered in this paper for reflective LPG, the fiber end facet is always coated with metal. We used commercially available FIMMWAVE Photon Design software, a fully-vectorial mode solver, to simulate the reflective LPG design. We considered the fiber parameters of commercially available SMF-28 fiber in our FIMMWAVE models and used the grating strength value of the proposed LPG of 3×10^{-4} [15].

3. Simulation results and discussions

The simulation results and associated discussions are organized in the following way. First, in section 3.1, based on our recent work [16], we discuss the effects of design parameters on the spectrum of a single reflective LPG. Next, in section 3.2, we present the simulation results for a distributed reflective LPG design and present the optimized design of a distributed reflective LPG structure that completely mimics the transmission spectrum shape over a 400 nm wide bandwidth.

3.1. Single reflective LPG

The effect of coating length and coating coverage on the reflected spectrum of a single LPG is discussed thoroughly and then the same principle is used to demonstrate the distributed reflected LPGs.

3.1.1. Effects of grating length on the reflected spectrum of LPG

We first studied the effect of the grating length (number of grating periods, N) on the reflected spectrum. For our chosen design parameters ($\Lambda = 390$ μm and grating strength of 3×10^{-4}), the core mode couples to LP_{05}, LP_{07}, LP_{09} cladding modes. This results in three discrete resonances at 1382 nm, 1406 nm, and 1558 nm, respectively, as shown in figure 2. The higher the order of the coupled cladding mode, higher is the sensitivity of the corresponding resonance wavelength to external parameters since higher order cladding modes are in close proximity to the interface between cladding and surrounding medium.

We increased the value of N from 25 to 65 in steps of 10. It is known from the coupled mode theory that the coupling strength depends on the refractive index contrast and the local variation of mode fields over a specific fiber length [17]. This can be seen from the simulated reflected spectra in figures 2(b)–(f) for $N = 25$–65, that with an increasing N, the resonance dips get narrower and deeper due to an increase in the coupling strength. However, the positions of the resonant dips remain unaltered. A reference transmission spectrum for $N = 45$ is shown in figure 2(a), and it can be seen that the transmission and the reflected spectra for $N = 45$ completely resemble each other in shape. Hence, for our studies throughout the paper, we choose a value of $N = 45$.

3.1.2. Effects of coating length on the reflected spectrum of LPG

For $N = 45$, we studied the effect of the metal coating length (L_c) on the reflected spectrum. To do this, we set $Lc = L_{end}$ and varied the coating length from $25\ \Lambda - 2550\ \Lambda$ in steps of $25\ \Lambda$. Only spectra for, $25\ \Lambda$, $725\ \Lambda$, $1450\ \Lambda$, $1800\ \Lambda$ and $2550\ \Lambda$ are shown figures 3(b)–(f). The simulated results indicate splitting in some of the resonant dips for a critical length $L_c < 1450\ \Lambda$. On the other hand, when $Lc \geqslant 1450\ \Lambda$, the reflected spectrum follows the transmission spectrum without any splitting. We hypothesize that the side coating effectively absorbs the coupled cladding modes beyond the critcal length of the coating while it propagates at the cladding/metal interface. Since the coupled cladding modes are absorbed by the metal coating, the LPG reflected spectrum does not show any interferometric fringes. However, a suitable coating length is highly required to absorb all the

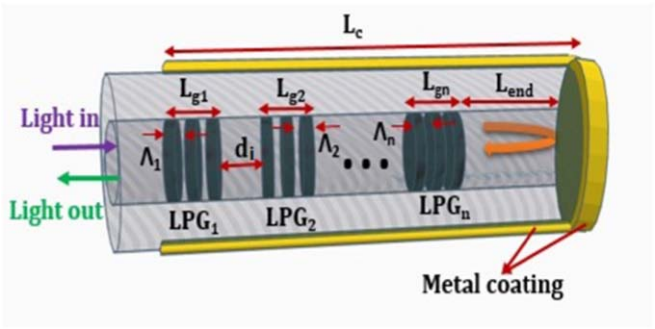

Figure 1. Schematic of a distributed reflective LPG sensor design comprising of *n* number of LPGs within a single fiber and all the designing parameters.

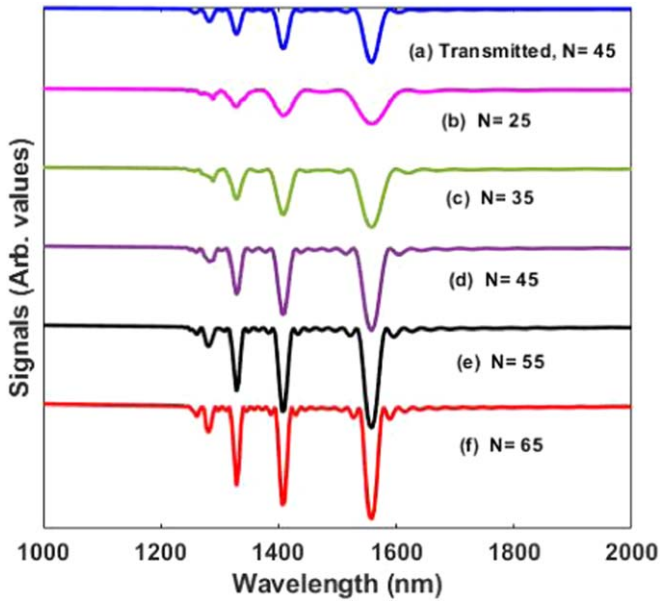

Figure 2. Spectrum of the designed LPG as a function of wavelength for different grating period numbers (*N*) for $n = 1$ and grating period of 390 μm: (a) transmitted spectrum and (b)–(f) reflected spectrum for $L_c = L_{end} = 1450\ \Lambda$.

coupled cladding modes. It can be said that coating length less than 1450 Λ is not sufficient to absorb all the coupled cladding modes, especially for operating over a wide bandwidth. The threshold value of the coating length beyond which the transmitted and reflected spectra mimic substantially was determined by calculating the correlation coefficient between these two spectra. We determined the coating length by setting a threshold correlation factor of 99.5% over which the reflected spectrum follows the transmitted spectrum completely. Therefore, we choose a value of $L_c = 1450\ \Lambda$ for our design.

Setting the value of $L_{end} = 1450\ \Lambda$, we further looked at the effect of varying the coating length from $L_c = 0$ to $L_c = L_{end} = 1450\ \Lambda$ on the reflected spectrum. It can be seen from the figures 4(b)–(d) that as the coating length is changed from 0 (figure 4(b)) to $L_{end}/2$ (figure 4(c)) to L_{end} (figure 4(d)), the reflected spectrum increasingly mimics the transmitted spectrum (figure 4(a)), where at 100%, the reflected and transmitted spectrum are identical over a 400 nm bandwidth.

In all cases in figure 4, the reflected spectra show reduced intensity but increased resonance depth compared to transmission spectrum.

3.1.3. Effects of coating coverage on the reflected spectrum of LPG

Finally, we studied the effects of coating coverage on the reflected spectrum for LPG with a grating period of $\Lambda = 390\ \mu$m. Figures 5(c)–(e) shows how the coating coverage changes the spectra from the optimized reflected spectrum ($L_c = L_{end} = 1450\ \Lambda$) (figure 5 (b)). It can be seen that for 25% coverage (figure 5(c)), the shape of the dip centered around 1558 nm starts to change and continues for 50% coverage (figure 5(d)) and completely

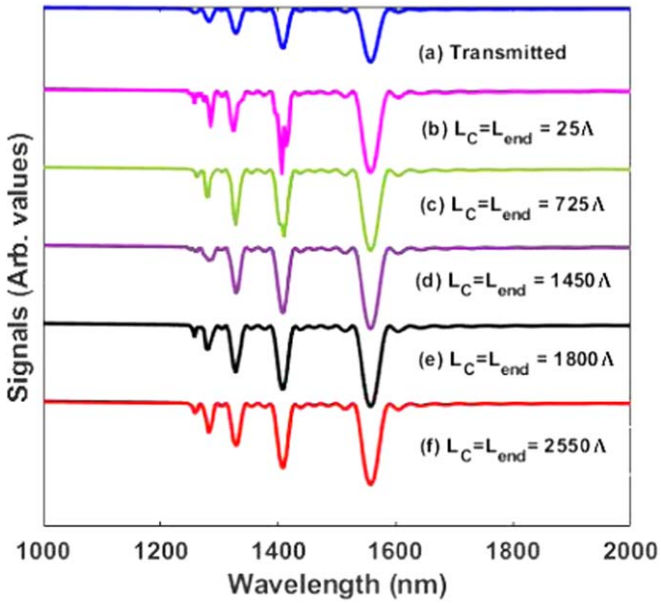

Figure 3. Effects of metal coating length on the reflected spectrum of the LPG for $n = 1, N = 45$ and grating period is of $\Lambda = 390$ μm: (a) transmitted spectrum and (b)–(f) reflected spectrum.

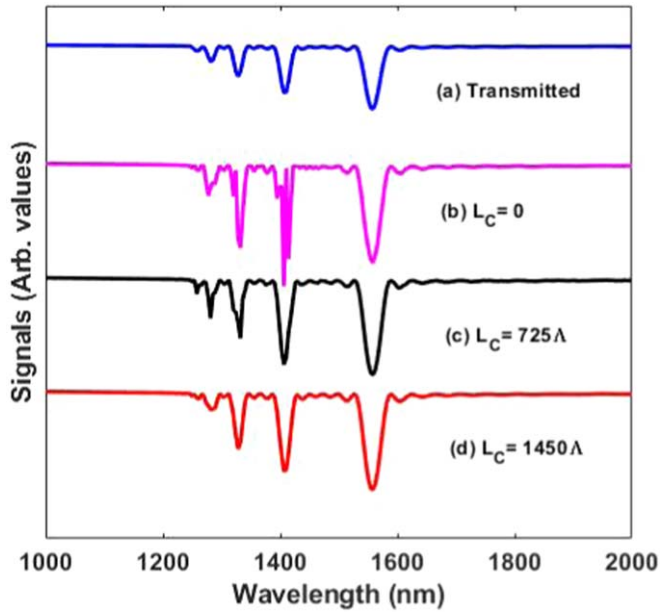

Figure 4. Effects of metal coating length on the reflected spectrum of the LPG for $n = 1, N = 45$ and grating period is of $\Lambda = 390$ μm while keeping the $L_{\text{end}} = 1450\Lambda$ fixed: (a) transmitted spectrum and (b)–(d) reflected spectrum.

vanishes for 75% and 100% coverage (figures (e), (f)). This happens because the metal coated directly over the grating influences the cladding modes, which in turn alters the coupling condition.

From the single reflective LPG simulations, we conclude that in order for the reflected spectrum to completely mimic the transmission spectrum shape over a large bandwidth, a coating length greater than 1450 Λ and a coating coverage of 0% are the optimal parameters.

3.2. Distributed reflective LPG

Next, we looked at the effect of including multiple LPGs within the same fiber on the reflected spectrum. For these simulations, we chose three LPGs with periods equal to $\Lambda_1 = \Lambda = 390$ μm (LPG1), $\Lambda_2 = 374$ μm (LPG2), and $\Lambda_3 = 346$ μm (LPG3) for designing a distributed reflective LPG with up to 3 different LPGs in a single fiber. Please note that LPGs are added from the end facet coating side and L_{end} is fixed at 1450 Λ_1. Just like for an LPG grating period of $\Lambda_1 = 390$ μm, we also performed simulations described in section 3.1 for grating periods of

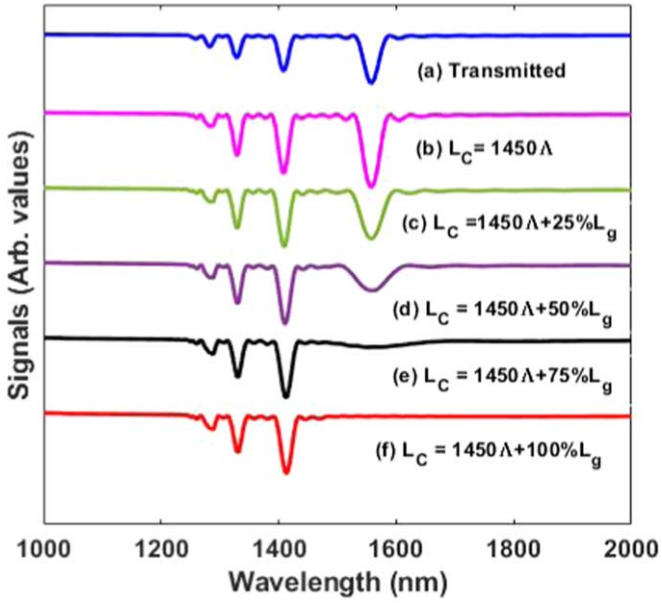

Figure 5. Effects of coating coverage on the spectrum of the designed LPG for $n = 1, N = 45$: (a) transmitted spectrum before inclusion of the metal coating, (c)–(f) reflected spectrum.

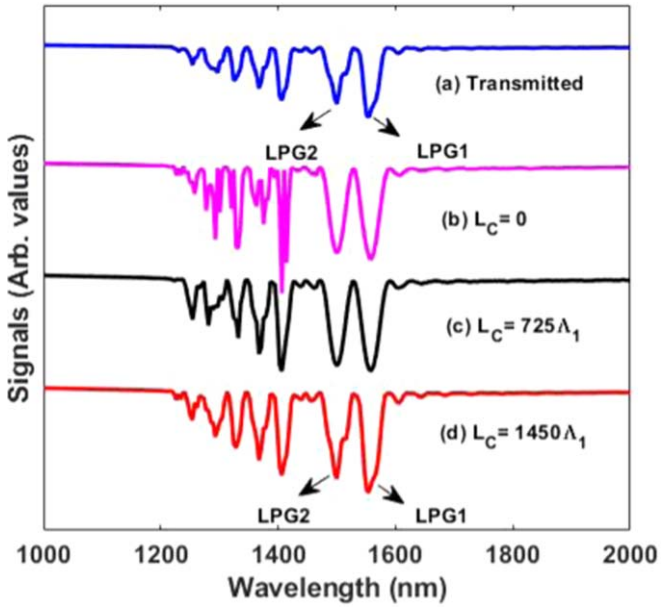

Figure 6. Effect of coating length on the reflected spectrum of the designed two LPGs ($n = 2$) added in series and $L_{end} = 1450\Lambda_1$ (a) transmitted spectrum before inclusion of the metal coating, (b)–(d) reflected spectrum.

and $\Lambda_2 = 374\,\mu$m and $\Lambda_3 = 346\,\mu$m. These simulations provided the same trends as those observed for the case of $\Lambda_1 = 390\,\mu$m period reflective LPG. Please note that the most higher order dips for grating periods of $\Lambda_1 = 390\,\mu$m, $\Lambda_2 = 374\,\mu$m, and $\Lambda_3 = 346\,\mu$m are centered around the wavelengths of 1558 nm 1500 nm, and 1400 nm, respectively

3.2.1. Effects of coating coverage and coating length for n = 2

We consider a simple case of a distributed reflective LPG design with two LPGs ($n = 2$). Figure 6(a) shows the simulated transmission spectrum when two LPGs with grating periods of $\Lambda_1 = \Lambda = 390\,\mu$m (LPG1), and $\Lambda_2 = 374\,\mu$m (LPG3) are included within the same fiber. L_{end} is fixed at 1450 Λ_1. Figures 6(b)–(d) show the effect of coating length on the LPG closest to the fiber facet ($\Lambda_1 = 390\,\mu$m) on the reflected spectrum. Similar to the effects observed in a single LPG case, when $L_c = L_{\text{end}} = 1450\,\Lambda_1$, the reflected spectrum mimics the transmitted spectrum completely. It can also be observed that dips for the higher order cladding modes are at

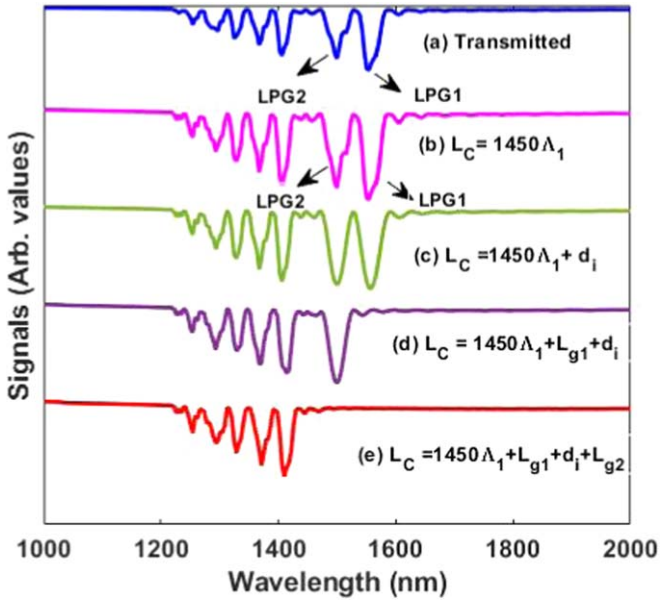

Figure 8. Spectrum of the cascaded two LPGs for different configurations for $n = 2$ and $N = 45$: (a) transmitted spectrum before inclusion of the metal coating, (b)–(e) reflected spectrum.

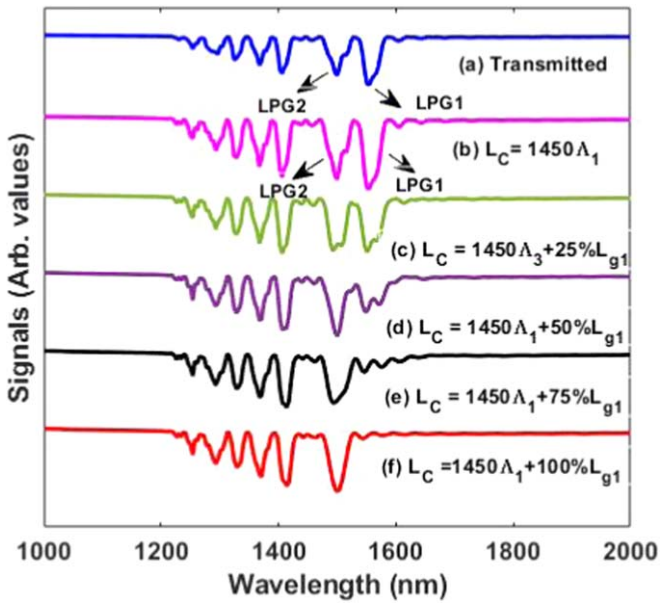

Figure 7. Effects of coating coverage on the spectrum of the designed LPG for $n = 2$ and $N = 45$: (a) transmitted spectrum before inclusion of the metal coating, (b)–(d) reflected spectrum.

wavelengths of 1558 nm and 1500 nm, which are also the dips for individual LPGs with grating period of $\Lambda_1 = 390\ \mu$m (LPG1) and $\Lambda_2 = 374\ \mu$m (LPG3), respectively. Figure 7 shows the effect of coating coverage on the LPG spectrum. It can be seen from figures 7(c)–(f) that similar to the single LPG case, coating coverage leads to splitting or disappearance of dips.

We also considered the effect of coating the metal over the length of the fiber between the two LPGs. Figures 8(c)–(e) show the effect of coating metal over different areas of the fiber for $L_{\text{end}} = 0$. $L_c = d$ (figure 8(c)), $L_c = L_{g1} + d$ (figure 8(d)), and $L_c = L_{g1} + d + L_{g2}$ (figure 8(e)), are the cases for when the metal is coated over the length between the gratings, the length between the gratings and over the last grating, and the length between the grating and both gratings, respectively. Please note that L_{g1} is the grating length of the LPG ($\Lambda_1 = 390\ \mu$m) closest to the end facet and L_{g2} is for $\Lambda_2 = 374\ \mu$m. Figure 8(b) shows the reflected spectrum for our optimized design parameters. It can be observed from figure 8(c) that while the dips for reflected spectrum are at the same wavelength as those for transmission spectrum on figure 8(a), the coating significantly affects the

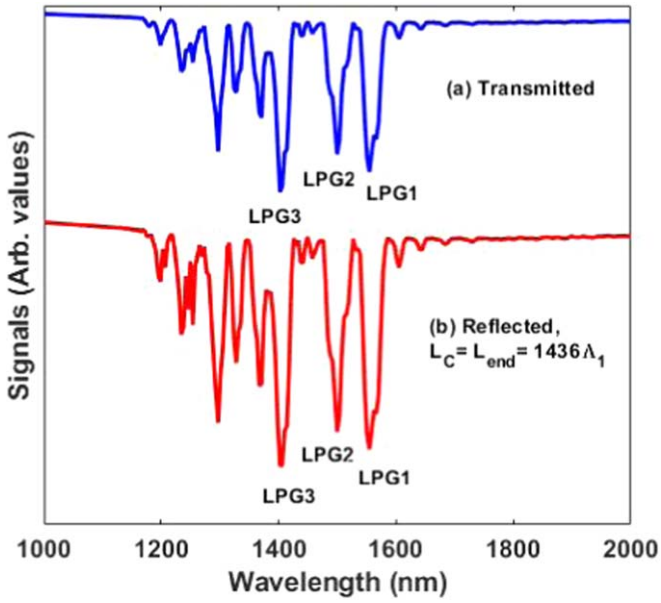

Figure 9. Spectrum of the cascaded three LPGs when $L_c = L_{end} = 1450\ \Lambda_3$ for $n = 3$ and $N = 45$ and grating period of $\Lambda_1 = 390$ μm, $\Lambda_2 = 374$ μm, and $\Lambda_3 = 346$ μm.

shape of the reflected spectrum. For these cases of figures 8(d)–(e), disappearance, and shifting of the dips can be observed, and the reflected spectra do not mimic the transmitted spectrum for any configuration. Thus, it can be concluded that the reflected spectrum follows the transmitted spectrum only when the metal coating is over the coating length $L_c = L_{\text{end}} \geqslant 1450\ \Lambda_1$ and is absent elsewhere.

3.2.2. Effects of coating coverage and coating length for $n = 3$

Simulation results from the single LPG and the dual cascaded LPGs indicate that $L_c = L_{end} \geqslant 1450\ \Lambda_1$ provides reflected spectrum that mimics the transmitted spectrum. Following this, a three cascaded reflection mode LPG is designed and simulated only *for* $L_c = L_{\text{end}} = 1450\ \Lambda_1$. Three LPGs with grating periods of $\Lambda_1 = 390$ μm (LPG1), $\Lambda_2 = 374$ μm (LPG2), and $\Lambda_3 = 346$ μm (LPG3) are added in a series, and the simulation results are shown in figure 9.

It can be seen that the reflected spectrum completely mimics the transmitted spectrum when $L_c = L_{end} = 1450\ \Lambda_1$ and no metal is coated anywhere else. Thus, we have generated an optimized design solution for a distributed reflective LPG comprising of multiple LPGs. Since the designed triple cascaded LPGs consists of these three grating periods, it is expected that it will couple light at wavelengths of 1558 nm, 1500 nm and 1400 nm. It can be seen from figure 9 that dips for the higher order cladding modes are at wavelengths of 1558 nm, 1500 nm and 1400 nm as expected.

4. Conclusion

In conclusion, in this paper, the effects of metal coating parameters on the spectrum of reflective LPGs for $n = 1$, 2, and 3 number of gratings in a single fiber have been presented. Coating metal over the grating or over any region between the LPGs either splits or leads to disappearance of some of the dips since it influences the cladding modes directly, and therefore, changes the coupling conditions. On the other hand, coating the tail end after the last LPG alone with metal provides a reflected spectrum that completely mimics the transmitted spectrum. The design methodology presented in this paper can be applied to a distributed sensor design comprising of n number of cascaded LPGs

Acknowledgments

This work was supported in part through the Department of Energy In-Pile Instrumentation program under DOE Idaho Operations Office Contract DE-AC07-05ID14517. The views and opinions of authors expressed herein do not necessarily state or reflect those of the US Government or any agency thereof.

ORCID iDs

Sohel Rana https://orcid.org/0000-0002-6281-3555

References

[1] James S W and Tatam R P 2003 Optical fibre long-period grating sensors: characteristics and application *Meas. Sci. Technol.* **14** R49
[2] Khaliq S, James S W and R P Tatam R P 2002 Enhanced sensitivity fibre optic long period grating temperature sensor *Meas. Sci. Technol.* **13** 792
[3] Hou R, Ghassemlooy Z, Hassan A, Lu C and K P Dowker K P 2001 Modelling of long-period fibre grating response to refractive index higher than that of cladding *Meas. Sci. Technol.* **12** 1709
[4] Bhatia V 1999 Applications of long-period gratings to single and multi-parameter sensing *Opt. Express* **4** 45–466
[5] Gwandu B A L 2002 Simultaneous refractive index and temperature measurement using cascaded long-period grating in double-cladding fibre *Electron. Lett* **38** 695–6
[6] Hromadka J, Korposh S, Partridge M C, James S W, Davis F, Crump D and Tatam R P 2017 Multi-parameter measurements using optical fibre long period gratings for indoor air quality monitoring *Sens. Actuators B Chem.* **244** 217–25
[7] Zawisza R, Eftimov T, Mikulic P, Bock W J and Jaroszewicz L R 2018 Ambient refractive-index measurement with simultaneous temperature monitoring based on a dual-resonance long-period grating inside a fiber loop mirror structure *Sensors* **18** 2370
[8] Esposito F, Srivastava A, Iadicicco A and Campopiano S 2019 Multi-parameter sensor based on single long period grating in Panda fiber for the simultaneous measurement of SRI, temperature and strain *Opt. Laser Technol.* **113** 198–203
[9] Ferreira M F *et al* 2017 Roadmap on optical sensors *J. Opt.* **19** 083001
[10] Allsop T, Reeves R, Webb D J, Bennion I and Neal R 2002 A high sensitivity refractometer based upon a long period grating Mach–Zehnder interferometer *Rev. Sci. Instrum.* **73** 1702–5
[11] Swart P L 2004 Long-period grating Michelson refractometric sensor *Meas. Sci. Technol.* **15** 1576
[12] Jiang M, Zhang A P, Wang Y C, Tam H Y and He S 2009 Fabrication of a compact reflective long-period grating sensor with a cladding-mode-selective fiber end-face mirror *Opt. Express* **17** 17976–17976
[13] Coelho T V N, Carvalho J P, Pontes M J, Santos J L and Guerreiro A 2013 A remote long-period grating sensor with electrical interrogation assisted by Raman amplification *Opt. Laser Technol.* **47** 107–13
[14] Qi L, Zhao C L, Yuan J, Ye M, Wang J, Zhang Z and Jin S 2014 Highly reflective long period fiber grating sensor and its application in refractive index sensing *Sens. Actuators B Chem.* **193** 185–9
[15] Biswas P, Basumallick N, Bandyopadhyay S, Dasgupta K, Ghosh A and Bandyopadhyay S 2014 Sensitivity enhancement of turn-around-point long period gratings by tuning initial coupling condition *IEEE Sens. Journal* **15** 1240–5
[16] Rana S, Subbaraman H and Kandadai N 2019 Role of metal coating parameters on the reflective long period grating spectrum *Optical Sensors and Sensing Congress (ES, FTS, HISE, Sensors)* p ETh1A.5 https://www.osapublishing.org/abstract.cfm?uri=ES-2019-ETh1A.5
[17] Fan P, Sun L P, Yu Z, Li J, Wu C and Guan B O 2016 Higher-order diffraction of long-period microfiber gratings realized by arc discharge method *Opt. Express* **24** 25380–8